

THE DEEP2 GALAXY REDSHIFT SURVEY: SPECTRAL CLASSIFICATION OF GALAXIES AT $Z \sim 1$

DARREN S. MADGWICK¹, ALISON L. COIL¹, CHRISTOPHER J. CONSELICE², MICHAEL C. COOPER¹, MARC DAVIS¹, RICHARD S. ELLIS², SANDY M. FABER³, DOUGLAS P. FINKBEINER⁴, BRIAN GERKE¹, PURAGRA GUHATHAKURTA^{3,5}, NICK KAISER⁶, DAVID C. KOO³, JEFFREY A. NEWMAN¹, ANDREW C. PHILLIPS³, CHARLES C. STEIDEL², BENJAMIN J. WEINER³, CHRISTOPHER N. A. WILLMER³, R. YAN¹ (THE DEEP2 SURVEY TEAM)

Draft version February 7, 2020

ABSTRACT

We present a Principal Component Analysis (PCA)-based spectral classification, η , for the first 5600 galaxies observed in the DEEP2 Redshift Survey. This parameter provides a very pronounced separation between absorption and emission dominated galaxy spectra – corresponding to passively evolving and actively star-forming galaxies in the survey respectively. In addition it is shown that despite the high resolution of the observed spectra, this parameter alone can be used to quite accurately reconstruct any given galaxy spectrum, suggesting there are not many ‘degrees of freedom’ in the observed spectra of the galaxy population. It is argued that this form of classification, η , will be particularly valuable in making future comparisons between high and low-redshift galaxy surveys for which very large spectroscopic samples are now readily available, particularly when used in conjunction with high-resolution spectral synthesis models which will be made public in the near future. We also discuss the relative advantages of this approach to distant galaxy classification compared to other methods such as colors and morphologies. Finally, we compare the classification derived here with that adopted for the 2dF Galaxy Redshift Survey and use this to show the importance of comparing similarly selected samples of galaxies when carrying out studies of evolution.

Subject headings: Galaxies: high-redshift — galaxies: evolution

1. INTRODUCTION

The classification of galaxies is of fundamental importance for understanding galaxy populations, and for this reason is a very important aspect of any galaxy redshift survey. Having a data set of many thousands of galaxy spectra allows one to test the validity of galaxy formation and evolution scenarios with unprecedented accuracy. However, the sheer size of the full spectral data set presents its own unique problems. In order to make such a galaxy data set more ‘digestible’ some form of data compression is necessary, whether this be through the adoption of morphological classification, colors or some other compression/classification scheme. If these quantities can be determined consistently over a wide range of redshifts, they can be compared with theoretical predictions and simulations, and hence set constraints on scenarios for galaxy evolution. This will be especially true if consistent classification regimes can be used for both the high redshift ($z \sim 1$) surveys currently underway (the DEEP2 Galaxy Redshift Survey, Davis et al. 2002 and the VIRMOS-VLT Deep Survey, Le Fevre et al. 1999) – and the large $z \sim 0$ surveys now approach-

ing full completion; the Sloan Digital Sky Survey (SDSS, Strauss et al. 2002) and the 2dF Galaxy Redshift Survey (2dFGRS, Colless et al. 2001)

A number of different approaches to the classification of galaxy spectra have been adopted for local galaxy surveys. These include the calculation of rest-frame colors (e.g. Strateva et al. 2001); principal component analysis (PCA) based spectral classifications (e.g. Connolly et al. 1995; Bromley et al. 1998; Folkes et al. 1999; Madgwick et al. 2002; de Lapparent et al. 2003), and other more sophisticated discriminations (e.g. Heavens, Jimenez & Lahav 2000; Slonim et al. 2001), based upon information theory. The underlying theme of all these alternative methods is that they characterize the galaxy population exclusively in terms of their observed spectra. The work presented here is the first attempt to apply one of these methods (PCA) to the classification of such a distant sample of galaxies.

1.1. The role of spectral classification

There are three methods which have generally proved to be popular for the classification of galaxies: morphological classification, rest-frame colors and direct spectrum based classifications. Each of these methods has its own unique drawbacks and advantages.

To understand galaxy evolution out to redshifts of $z \gtrsim 1$, it is essential to have a consistent implementation of these classifications over a wide range of look-back times. For this reason it can be argued that morphological segregation – although perhaps the most natural form of classification – may not be the optimal solution to adopt over such a large range of redshifts. This is due to both the degradation of morphology with redshift and the absence of a robust and repeatable methodology to

¹ Department of Astronomy, University of California, Berkeley, CA 94720

² Department of Astronomy, California Institute of Technology, Pasadena, CA 91125

³ University of California Observatories/Lick Observatory, Department of Astronomy and Astrophysics, University of California, Santa Cruz, CA 95064

⁴ Princeton University Observatory, Princeton, NJ 08544

⁵ Herzberg Institute of Astrophysics, National Research Council of Canada, 5071 West Saanich Road, Victoria, B. C., Canada V9E 2E7

⁶ Institute for Astronomy, University of Hawaii, Honolulu, HI 96822

perform this classification (see e.g. Conselice 2003 for further discussion and possible solutions to this situation). For this reason we focus in this paper on alternative classification methods to morphology, which we hope will complement earlier studies based on this method, whilst at the same time providing a new perspective by more directly reflecting the physical properties of each galaxy.

The remaining two options – rest-frame colors and spectral ‘types’ – are linked, in that they both provide some compressed representation of the observed galaxy’s spectral energy distribution (SED), hence providing a relatively direct insight into physical processes such as star-formation currently occurring in each galaxy. However, in terms of how each is calculated for high- z galaxies there are significant differences which are important to understand.

The main complication for the calculation of rest-frame colors is the accurate determination of k -corrections to account for the different pass-bands sampled by each photometric filter at different redshifts. These generally cannot be estimated from the observed spectrum, but rather must be determined by matching each observed galaxy to a set of template SEDs with full rest-frame wavelength coverage.

In the case of spectral classification, one must consider that the rest-frame wavelength coverage varies with the redshift of the galaxy, hence to adopt a uniform classification over a large range of redshifts one needs to significantly restrict the rest-frame wavelength range considered (e.g. by focusing in on particular line features through equivalent width measurements) or to determine some way of filling in the gaps that are not observed in each spectrum.

These two problems are very closely related in that they express the need to determine the form of a galaxy’s SED over a wavelength interval that is not necessarily observed. In the case of k -corrections only ~ 10 template SEDs are available for this task (Kinney et al. 1996; Coleman, Wu & Weedman 1980); reddening is manually incorporated. However as will be shown in this paper, with principal component analysis (PCA), we can achieve this same task for spectral classification, using the observed spectra themselves as templates, giving us $\sim N_{\text{gal}}$ galaxy templates.

For this reason adopting PCA-based spectral types will provide a classification scheme that is particularly uniform over the large range of redshifts encountered in the DEEP2 redshift survey, hence providing a robust probe of evolution in the galaxy population. In addition we note that such methods of classification are timely, in that there is now a considerable body of low redshift spectroscopic data from e.g. 2dFGRS and SDSS, which enables us to make detailed comparisons. We note that PCA-based classifications do suffer from one particular drawback, which is that they are not as straightforward to interpret as other classifications, and this is an issue we will attempt to address in this paper.

The outline of this paper is as follows: In Section 2 we briefly discuss the DEEP2 Redshift Survey data that we will use in this analysis. Section 3 describes the implementation of PCA we have adopted for this paper, and gives a discussion as to why this particular formalism has been used. In particular, issues regarding the rest-

frame wavelength coverage are discussed in some detail. In Section 4 we discuss the method of spectral classification we will adopt, based upon the results of the PCA we have implemented. This spectral classification is contrasted with that of the 2dF Galaxy Redshift Survey in Section 5, in which the selection effects of the two surveys are also discussed. We then conclude this paper in Section 6 with a brief discussion as to future applications of this work.

2. DEEP2 GALAXY SPECTRA

In its first season of observations (August – October, 2003), the DEEP2 Redshift Survey has already accurately measured the redshifts of ~ 5600 galaxies, out of a proposed total of 60,000. These galaxies have been pre-selected to have $z \gtrsim 0.7$ and an R_{AB} limiting magnitude of 24.1, from a set of B, R and I CFHT 12k x 8k images covering $\sim 4 \text{ deg}^2$ on the sky. Foreground galaxies have been excluded using a simple photometric cut, based upon the observed $R - I$ and $B - R$ color of each galaxy (Davis et al. 2002). In this paper we make use of all this data from the first observing season.

A sophisticated automated pipeline has been developed to efficiently extract and reduce the spectra observed in the survey, details of which will be presented by Davis et al. (2003). The observed spectra themselves are taken at high resolution ($R \sim 5000$) using the DEIMOS spectrograph mounted on the 10-m Keck-II telescope (Davis & Faber, 1998), and generally span the wavelength range of $6400 < \lambda < 9200 \text{ \AA}$. For galaxies with $z > 0.7$ this allows us to very accurately measure the redshift of each galaxy, particularly when the resolved [OII] doublet is present (out to a redshift of $z = 1.5$). Absorption based redshifts are also readily determined, primarily using the Ca H+K features which are visible to redshifts of $z \sim 1.3$.

All spectra used in this analysis have been corrected for the DEIMOS throughput efficiency of the 1200 line/mm grating used in the survey⁷, and are presented in units of counts/pixel/hour. Note that the flux calibration is only approximate at present, however we have found the components derived from our PCA to be robust to the exact value of the throughput efficiency. Additionally, the spectra have been normalized to have a mean count of unity, after being minimally smoothed (3 pixels $\sim 0.9 \text{ \AA}$ observed-frame, $\sim 0.5 \text{ \AA}$ restframe) according to the inverse of their estimated variance (in order to remove sky residuals and other artifacts remaining from the spectral reduction).

3. PRINCIPAL COMPONENT ANALYSIS

The spectral classification presented here is based upon a Principal Component Analysis (PCA) of the DEEP2 galaxy spectra. PCA is a powerful technique, allowing us to easily visualize and quantify a multi-dimensional population in terms of just a handful of significant components. It does this by identifying the components of a data set (in this case the galaxy spectra) which are the most discriminatory between each galaxy (where the significance is determined in terms of its contribution to the variance over the entire sample). This allows us to identify just the most significant components for future use.

⁷ see <http://www.ucolick.org/~ripisc/Go1200.html>

It is clear from such a formalism that any clustering in the PCA space is indicative of distinct sub-populations within the sample.

PCA has been used with considerable success by a variety of authors to deal with large multi-dimensional data sets. Several similar mathematical formulations of PCA for galaxy spectra have appeared in the literature, in particular Connolly et al. (1995); Bromley et al. (1998); Galaz & de Lapparent (1998); Folkes et al. (1999). The most significant difference between the various techniques is that some methods utilize mean-subtracted covariance matrices for the PCA (by subtracting the mean of the normalized spectrum of each galaxy), while others do not. This has little effect on the subsequent analysis since the latter methods simply yield a mean spectrum as the first component.

In this paper we present a new variation on previous formalisms for carrying out the PCA of galaxy spectra, designed to accommodate the features of our data set that make the standard method very difficult to apply. In particular there are two complications that must be addressed to analyze the DEEP2 galaxy spectra: the first is the very high resolution of the observed spectra which require extremely time-consuming matrix computations. The second is that the observed spectra cover very different rest-frame wavelength ranges once de-redshifted.

3.1. Implementing PCA for high-resolution data

A significant drawback to implementing PCA on large or very high-dimensional data sets is the required computation time, particularly to determine the covariance matrix. For n galaxies - each with p spectral channels - this requires $O(np^2)$ operations. Given that each DEEP2 spectrum contains $O(10^4)$ channels this would be very time consuming indeed if the full spectral resolution is used.

Fortunately, it is possible to solve for the PCA eigenspectra without calculating the entire covariance matrix. The key is developing a probabilistic formalism for the PCA, compatible with an expectation-maximization (E-M) algorithm (see Roweis 1997 and Tipping & Bishop 1999). Adopting such a formalism allows one to solve for the first k eigenspectra in only $O(npk)$ operations. It has been shown that this method for performing PCA is robust, in that it has only one stationary point that is not a saddle point, which guarantees there will be no false convergences (Tipping & Bishop 1999).

Computationally, the E-M algorithm proceeds in iterations of two steps. The k eigenvectors to be calculated are assumed to be spanned by the columns of a $p \times k$ matrix \mathbf{C} . We start by making an initial (random) guess for the columns of this matrix and use this to determine the $k \times n$ matrix, \mathbf{X} , of k 'states' for each galaxy. These states correspond to the principal component projections of each galaxy in the non-orthogonal space defined by the columns of \mathbf{C} . These states are then used in conjunction with the original $p \times n$ data matrix, \mathbf{Y} , to make a better estimate for \mathbf{C} . This proceeds until convergence. These steps can be summarized as,

1. Step I:

$$\mathbf{X} = (\mathbf{C}^T \mathbf{C})^{-1} \mathbf{C}^T \mathbf{Y}$$

2. Step II:

$$\mathbf{C}^{\text{new}} = \mathbf{Y} \mathbf{X}^T (\mathbf{X} \mathbf{X}^T)^{-1}$$

Once the algorithm converges the columns of \mathbf{C} will span the space of the first k eigenvectors. This can therefore be used to construct the orthogonal basis that defines the principal components and their projections. We note that this method for PCA gives identical principal components to the other (simpler) formalisms discussed previously. The sole reason we adopt an E-M based approach is to make the PCA efficient for the large and very high resolution data set we are using. Throughout the remainder of this paper we will denote the eigenvectors determined by the PCA (herein eigenspectra) as $\mathbf{P}_1, \mathbf{P}_2$ etc. and the projections onto these axes by p_1, p_2 etc.

3.2. Dealing with incomplete data in the PCA

The treatment of incomplete data in PCA has already been discussed in the literature, e.g. Everson & Sirovich (1995) and Connolly & Szalay (1999). However, the implementation is complicated and deserves further discussion. The issues that must be resolved are two-fold: First, how to determine the eigenspectra (or principal components) when very few galaxies cover the full wavelength range, and second, how to project a galaxy onto these eigenspectra when its spectrum does not cover the entire restframe wavelength range considered. It can be shown that the latter issue has a relatively straightforward, clean solution involving de-correlating the eigenspectra (which are not orthogonal when we do not use their entire wavelength coverage). This has been presented in Connolly & Szalay (1999). However, estimating the eigenspectra in the first place is much more difficult to address.

Consider the situation when the eigenspectra, \mathbf{P}_i , have already been estimated using the PCA. Each of the observed, mean-subtracted spectra, $\mathbf{f}' = \mathbf{f} - \bar{\mathbf{f}}$, can then be expressed as a linear combination of these eigenspectra,

$$\mathbf{f}' = \sum_i p_i \mathbf{P}_i, \quad (1)$$

where $\bar{\mathbf{f}}$ is the mean spectrum of all the galaxies and $p_i = \mathbf{f}' \cdot \mathbf{P}_i$ is the projection of each galaxy onto the i th principal component. The index i ranges from 1 to the number of resolution elements in each spectrum. However, because most of the variance in each spectrum is contained in only the first few eigenspectra (as will be demonstrated later), the sum in Eqn. 1 can be truncated to include only the first k most significant elements.

We wish to determine how to derive the projections p_i when the spectrum, \mathbf{f}' , does not cover the full restframe wavelength range spanned by the eigenspectra (e.g. because of poor sky subtraction or the effects of redshift). The eigenspectra are defined to be orthonormal,

$$\mathbf{P}_i \cdot \mathbf{P}_j = \delta_{ij}. \quad (2)$$

However, when we only consider the wavelength range over which the observed spectrum, \mathbf{f}' , is defined this is no longer the case. We denote the incomplete spectrum by $\mathbf{w}\mathbf{f}'$, where \mathbf{w} is a vector with non-zero elements only where \mathbf{f}' is defined. As shown in Connolly & Szalay (1999), the correlations between the portions of the

eigenspectra relevant for f' can be quantified in terms of a correlation matrix,

$$\mathbf{M}_{ij} = \mathbf{wP}_i \cdot \mathbf{P}_j. \quad (3)$$

Using this matrix it is possible to show that, when a spectrum does not cover the entire wavelength range of the eigenspectra, unbiased estimates of the true projections can be calculated using the formula,

$$\hat{p}_i = \sum_j \mathbf{M}_{ij}^{-1} \mathbf{P}_j, \quad (4)$$

where again this sum need only be carried out over the most significant principal components (in our case we will use the first $k = 20$). In what follows we use this procedure for two separate purposes: to estimate the *corrected* projections, \hat{p}_i , when the wavelength range of the galaxy does not fully span the eigenspectra, and (using these corrected projections) to interpolate over any gaps in a spectrum resulting from sky-subtraction etc., using Eqn. 1. This is discussed further in the next section.

Before this formalism can be adopted one first requires an estimate of the eigenvectors of the PCA, \mathbf{P}_i . Several approaches to estimating these eigenspectra in cases where few or no galaxies cover the full wavelength range of interest have been suggested. Everson & Sirovich (1995) discuss approaches involving extrapolation of the observed spectra followed by iteration. Another approach is to make a least-squares generalization to the E-M PCA (Roweis 1997). Each of these methods assumes that the ‘gaps’ in each spectrum are randomly positioned, which may be true of low- z galaxy spectra but is clearly unsatisfactory for high- z surveys since almost all of the observed spectra will miss a substantial amount of either the extreme blue or extreme red end of the full rest-frame wavelength range. For this reason a simple approach to estimating the eigenspectra will normally fail, since it is difficult to correlate (and hence extrapolate) one end of the observed spectrum with what would be expected at the other end.

A more practical solution, which we follow in this paper, is to restrict the rest-frame wavelength range of interest such that there is a more significant subsample of galaxies which span the entire wavelength range of interest. Two such divisions are outlined in Fig. 1; the first involves considering only the rest-frame wavelength range of 3700-4200Å (covering [OII] and beyond the 4000Å break) while the second is extended to 3700-5050 Å (essentially covering [OII] to [OIII]). There is an obvious draw-back to this approach in that we are not making use of all the information contained in our observed spectra; however, as will be shown below this is a necessary compromise.

3.3. Limited λ PCA

Using the first wavelength cut (3700-4200Å), $\sim 50\%$ of our galaxy sample span the entire rest-frame wavelength range (with the exception of small gaps masked out due to bad sky subtraction, gaps between the CCDs and bad pixels) and can be used in a PCA analysis. For the second wavelength cut (3700-5050Å), we are using a greater portion of the observed galaxy spectra and so the analysis is potentially more informative; however, only $\sim 10\%$ of galaxies span this entire wavelength range.

In each case the procedure we adopt is as follows:

1. The subset of our galaxies which span the entire restframe wavelength range of interest are passed through the E-M PCA to determine a first set of $k = 20$ eigenspectra, corresponding to the orthogonalized columns of the matrix \mathbf{C} (c.f. Section 3.1).
2. Small gaps in the galaxy spectra used in the previous step are interpolated over by re-calculating the ‘de-correlated’ projections, \hat{p}_i (as described in the previous section) and are then used to reconstruct the missing parts of the spectrum. The new galaxy spectra are then re-processed through the PCA to produce improved estimates of the PCA eigenspectra.
3. The new set of eigenspectra is then used to compute projections for the entire galaxy sample regardless of rest-frame wavelength coverage, by means of the de-correlation procedure outlined in Sec. 3.2.

We do not iterate further after projections have been determined for the entire galaxy sample, since this tends to propagate errors through the analysis and can lead to unphysical eigenspectra.

The values of the first two projections derived in this manner are plotted in Fig. 2, for both the rest-frame wavelength ranges considered. This figure allows us to determine whether the PCA is robust beyond the narrow redshift range that corresponds to each of the rest-frame wavelength limits adopted. To judge this we have compared in each case the distribution of the first two components (p_1 and p_2) for only those galaxies used in the initial PCA (the *restricted* z sample), and those for the entire galaxy sample (the *unrestricted* z sample). Although some small degree of systematic offset is expected, the two should be broadly similar, which is clearly not the case for the second sample used (3700-5050Å). This lack of agreement effectively highlights the limitations of performing PCA for spectra that do not have a sufficient degree of overlap.

Clearly the extended sample is more interesting, in so far as it covers a larger rest-frame wavelength range and therefore includes more spectral features. However, Fig. 2 demonstrates that this classification cannot in fact be performed robustly since too few galaxies cover this full rest-frame wavelength range. On the other hand, the more restricted wavelength choice (3700-4200Å) is much more robust. We therefore choose to adopt this latter wavelength coverage to define our spectral classification.

4. SPECTRAL CLASSIFICATION

PCA is not a classification algorithm, rather, it is simply a method of data compression. For this reason another (usually manual) step must be performed, in which the insight gained from this compression is used to divide a galaxy sample. This is not necessarily straightforward and will usually involve some degree of arbitrariness – especially since galaxy spectra appear to span a single continuum of types rather than falling into distinct classes.

By far the most significant output of the PCA is the first principal component (p_1 contains 10 times more variance than any other component in our analysis, see Fig. 3), which appears to be dominated by the nebular emission line strengths in a spectrum. In particular the strength of the [OII] emission feature figures prominently,

as shown in Fig. 4. Note however that, as demonstrated in Fig. 3, this component does in fact also encapsulate a great deal more information about each spectrum and can be used to very accurately reconstruct a wide variety of galaxy spectra.

Other eigenspectra, examples of which are shown in Fig. 4, also contain useful information about each spectrum. For example, the second eigenspectrum, \mathbf{P}_2 , appears to primarily quantify the width of the various emission lines that is not incorporated into the first principal component. The component \mathbf{P}_3 reflects the stellar continuum, and in particular the height of the 4000Å break relative to [OII] that is not already encapsulated in the first principal component. Note that each of these eigenspectra represent variations in the galaxy spectra relative to the mean spectrum and so, for example, the [OII] line in \mathbf{P}_1 represents the additional emission line strength present in each spectrum, whether this be less than ($p_1 < 0$) or greater than ($p_1 > 0$) the value for the mean spectrum. Beyond the fourth principal component the eigenspectra become dominated by unphysical features in the galaxy spectra.

Because the first component is so much more discriminatory between galaxies (in terms of variance) this appears to be the most logical (and simplest) classification to adopt, particularly since this component alone appears to do well at reconstructing a large variety of observed spectra. It is additionally reassuring to note that \mathbf{P}_1 also encapsulates the greatest variety of features in each galaxy’s spectrum (Fig. 4), and so is also potentially the most astrophysically interesting component available from the PCA.

A similar dominance of the first principal component, p_1 , has been noted in previous analyses of low- z galaxy surveys, suggesting that the distribution of ‘normal’ galaxy spectra can be well approximated by a one dimensional sequence. However, we must be careful to ensure that this projection is in fact a robust measure of a galaxy’s spectrum if we are to use it alone to determine spectral type. For example, it has been noted for low- z galaxy samples observed through small fiber optic apertures that the first principal component was not stable between multiple observations of the same object (Bromley et al. 1998; Madgwick et al. 2002). We find that this is not the case for our most significant projections, which proved to be relatively robust (for example the 1σ deviation in p_1 between repeated observations of the same object is only $\sigma_{p_1} \sim 5$), most likely owing to the use of slit-apertures instead of fiber optics. We therefore choose to adopt p_1 as our measure of spectral type for galaxies observed in the DEEP2 Redshift Survey and denote it by,

$$\eta_{\text{DEEP}} \equiv p_1. \quad (5)$$

This notation has been specifically chosen to analogous to low redshift samples (e.g. the 2dFGRS) for which a similar classification scheme has been adopted.⁸

⁸ Note that in the 2dFGRS, η was defined as a linear combination of the first *two* components; p_1 and p_2 . The two components were needed because of the additional calibration uncertainties introduced by the small fiber apertures used in that survey. Despite this the classifications are in fact comparable as that combination was also the most statistically significant output of the PCA which was robust to the known instrumental uncertainties.

A histogram of η is shown in Fig. 5, in which a significant bimodality appears to be present. Since this is the only discontinuity in the distribution of this projection, it is natural to divide the sample there ($\eta \sim -13$). The presence of this bimodality is interesting in that similar effects have been observed with galaxy colors (Strateva et al. 2001; Bell et al. 2003; Weiner et al. 2003) and also in spectral classifications of other samples such as in the 2dFGRS (Madgwick et al. 2002).

Having divided the galaxies into two ‘types’, we proceed to calculate the mean spectrum for each type, shown in Fig. 6. Clearly, the difference between these two classes is quite pronounced, and is differentiating primarily between absorption spectra (associated with older stellar populations) and emission dominated spectra (associated with recent star-formation activity). Taking this interpretation further, it should be possible to directly relate this classification to the underlying star-formation activity in each galaxy as was done for the 2dFGRS (see Madgwick et al. 2003). We return to this point in Sec. 5. Galaxies with values of η less than -13 will be referred to as either ‘early type’ or passively evolving galaxies, whilst those with higher values will be referred to as ‘late type’ or actively star-forming galaxies.

Figure 7 shows the observed distribution of $(R-I)$ and $(B-R)$ colors for each type of galaxy, as defined by our η parameter. It can be seen from this figure that there is a very good separation between the galaxies in this plane of colors, suggesting a very tight correlation between color and the strength of emission/absorption features in each observed spectrum. An even more striking correspondence is seen in the rest-frame color distribution of the different types of galaxies, and this will be investigated further in a future paper.

5. COMPARISON WITH $Z = 0$ CLASSIFICATION

In this Section we briefly compare the classification derived for the DEEP2 Survey with that adopted in the 2dF Galaxy Redshift Survey (Colless et al. 2001), which comprises over 200,000 low redshift galaxy spectra. The reason we make this particular comparison is that the two classification regimes have been identically defined, in that they are both derived from the most significant component of the PCA that is robust to the known instrumental uncertainties (Madgwick et al. 2002). Such a classification for the Sloan Digital Sky Survey is also in progress but is not yet available.

The 2dFGRS has been selected using b_J magnitudes out to an extinction-corrected limit of ~ 19.5 . Because of the low redshifts of the galaxies used in this survey, these magnitudes correspond approximately to a rest-frame B selection ($\langle B - b_J \rangle \sim 0.09 \pm 0.01$). Selecting galaxies using restframe B magnitudes will preferentially select galaxies with recent episodes of star formation, particularly as compared with R selected samples such as the SDSS. Galaxies in the DEEP2 Survey have been selected using R magnitudes, which at $z \sim 1$ corresponds more closely to a restframe U selection of galaxies – which will be even more biased towards episodes of recent star formation.

Because almost all galaxies in the DEEP2 Survey have an observed color of $R - I < 1.5$, a fair comparison between this survey and the 2dFGRS can be made by drawing an $I < 22.6$ magnitude limited subsample from the DEEP2 survey. Because the magnitude limit of the

spectroscopic sample is defined to be $R = 24.1$, this I -selected subsample should be highly complete, and will correspond much more closely to a purely restframe B selection over the redshift interval $0.7 < z < 1.0$ (see e.g. Lilly et al. 1995).

We note that in order to make the detailed comparisons between different galaxy surveys – particularly those at different redshifts – much more careful assessments of these selection criteria will be necessary, most likely involving an incorporation of the galaxy luminosity functions from each survey. However, in what follows we proceed by assuming that the galaxy selection criteria are similar enough for a rough comparison between the two populations and leave a more detailed comparison of the populations for a subsequent publication.

Both classification methods provide a continuous parameterization of the spectral type of a galaxy, denoted by η . However, because the DEEP2 survey spectra have much higher resolution, the locus of projections for this survey spans a much larger range. For this reason we scale the η_{2dF} spectral parameter of the 2dFGRS survey to match η_{DEEP} . We find that multiplying by a factor of 8 suffices to match the two classifications, a similar factor would be derived by noting that early type galaxies are separated from late types at $\eta_{2dF} = -1.4$ (Madgwick et al. 2002), as opposed to $\eta_{DEEP} = -13$.

In Fig. 8 we compare the distribution of spectral types for both the R and I -limited DEEP2 samples (corresponding to restframe U and B selection respectively), and for the I -limited DEEP2 and 2dFGRS samples. It can be seen that the distribution of spectral types in the restframe- B selected DEEP2 and 2dFGRS samples have a remarkably similar form, whereas there is a substantial difference between selecting galaxies in restframe U as opposed to B .

Figure 9 shows a comparison of the average spectra for early and late type galaxies as calculated from the 2dFGRS and DEEP2 spectra (with the latter smoothed to the 9\AA resolution of the former). This figure, together with comparison in the spectral type distribution, show that the correspondence between the two classifications is quite striking. Despite being derived over different wavelength ranges and at different resolutions, they essentially encapsulate the same physical information.

It has already been shown (Madgwick et al. 2003) that the spectral classification η adopted for the 2dFGRS corresponds most naturally to the relative amount of star formation activity currently occurring in each galaxy as compared with its past average (the Scalo birthrate, b , parameter, Scalo 1986). Objects with high η values are galaxies with particularly strong recent star formation, whereas the lowest- η sample of galaxies has $b \leq 0.1$ (i.e. their current star formation rate is only 10% of their past averaged value). Because there is such a simple one-to-one correspondence between the spectral classification and the star formation activity of each galaxy, we can confirm from Fig. 8 our intuition that selecting galaxies using restframe U magnitudes is very much more biased towards galaxies with recent episodes of star-formation than B selection. This result will have important repercussions for the interpretation of future analyses of the DEEP2 Survey data.

A more detailed assessment of the exact relative fre-

quency of star forming galaxies in each survey will be forthcoming in a future paper, in which the selection function of each survey will be fully incorporated. Once this is available it will also be particularly interesting to experiment with how consistent the evolution between the populations is with that expected from spectral synthesis models (e.g. Bruzual & Charlot 1993; Fioc & Rocca-Volmerange 1997).

6. CONCLUSIONS

In this paper we have presented a new PCA-based spectral classification, η_{DEEP} , for the galaxies observed to date in the DEEP2 Redshift Survey. The main goal in developing this classification was to provide a consistent and robust measure of the type of a galaxy over the large range of redshifts encountered in this survey. To do this special handling of incomplete and ‘gappy’ observed spectra is required.

Although this classification, η_{DEEP} , appears to primarily identify galaxies with differing strengths of nebular emission, Fig. 3 demonstrates that this component alone can reconstruct the spectra of a wide variety of galaxies extremely well.

We have not directly related this classification to the role of star formation activity in a given galaxy. However, there is strong evidence from a similar analysis carried out for the 2dFGRS that η_{DEEP} should also correlate well with the relative amount of star formation. A more detailed study of this correlation, together with the role of higher order PCA projections, will be forthcoming when higher resolution spectral synthesis models become publicly available in the near future (the DEEP2 galaxy spectra are at a resolution that is ~ 20 times higher than any synthesis model currently available).

This particular classification will be particularly useful in subsequent analyses e.g. of the galaxy luminosity function or correlation functions, as it is easily comparable with other classifications at $z = 0$, for which large spectroscopic samples are now publicly available. In addition, previous work (e.g. Madgwick et al. 2003) has shown that it is straightforward to make direct comparisons between such a spectral classification regime and the output of semi-analytic galaxy models (e.g. Kauffmann, White & Guiderdoni 1993; Cole et al. 1994; Somerville & Primack 1999), allowing us to directly constrain the assumed models of galaxy formation and evolution between $z = 1$ and $z = 0$ using this form of classification.

When used in conjunction with spectral synthesis models, we expect that parameters similar to the one presented here will provide a wealth of information on both the amount and ‘type’ of evolution that has occurred in the galaxy population. This is particularly relevant now that such large samples of galaxy spectra are becoming available over such a wide range of redshifts. For this reason we expect studies of the evolution in the galaxy population to become a particularly rich field of research in the near future, and that the DEEP2 Redshift Survey will play an especially prominent role in this field.

This work was supported in part by NSF grants AST00-71048 and KDI-9872979. The DEIMOS spectrograph was funded by a grant from CARA (Keck Observatory), by an NSF Facilities and Infrastructure grant (AST92-2540), by the Center for Particle Astrophysics,

and by gifts from Sun Microsystems and the Quantum Corporation. DPF is supported by a Hubble Fellowship. The DEEP2 Redshift Survey has been made possible

through the dedicated efforts of the DEIMOS staff at UC Santa Cruz who built the instrument and the Keck Observatory staff who have supported it on the telescope.

REFERENCES

- [1] Bell, E. F., Wolf, C., Meisenheimer, K., Rix, H-W., Borch, A., Dye, S., Kleinheinrich, M., McIntosh, D. H., 2003, ApJ submitted, astro-ph/0303394
- [2] Bromley, G. C., Press, W. H., Lin, H., Kirshner, R. P., 1998, ApJ, 505, 25
- [3] Bruzual, A. G., Charlot, S., 1993, ApJ, 405, 538
- [4] Cole, S., Aragon-Salamanca, A., Frenk, C. S., Navarro, J. F., Zepf, S. E., 1994, MNRAS, 271, 781
- [5] Coleman, C. D., Wu, C. C., Weedman, D. W., 1980, ApJS, 43, 393
- [6] Colless, M. M., et al., (*the 2dFGRS Team*) 2001, MNRAS, 328, 1039
- [7] Connolly, A. J., Szalay, A. S., Bershad, M. A., Kinney, A. L., Calzetti, D., 1995, AJ, 110, 1071
- [8] Connolly, A. J., Szalay, A. S., 1999, ApJ, 117, 2052
- [9] Conselice, C., 2003, ApJS accepted, astro-ph/0303065
- [10] Davis, M., Faber, S., 1998, 'Wide Field Surveys in Cosmology', IAP XIV, Eds. Colombi S., Mellier Y., Editions Frontieres, Paris
- [11] Davis, M., et al., (*the DEEP2 Team*) 2002, SPIE, astro-ph/0209419
- [12] Davis, M., et al., (*the DEEP2 Team*) 2003, in preparation
- [13] Everson, R., Sirovich, L., 1995, J. Opt. Soc. Am., 12, 8
- [14] Fioc, M., Rocca-Volmerange, B., 1997, A&A, 326, 950
- [15] Folkes, S., et al. (*the 2dFGRS Team*) 1999, MNRAS, 308, 459
- [16] Galaz, G., de Lapparent, V., 1998, A&A, 332, 459
- [17] Heavens, A. F., Jimenez, R., Lahav, O., 2000, MNRAS, 317, 965
- [18] Kauffmann, G., White, S. D. M., Guiderdoni, B., 1993, MNRAS, 264, 201
- [19] Kinney, A. L., Calzetti, D., Bohlin, R. C., McQuade, K., Storchi-Bergmann, T., Schmitt, H. R., 1996, ApJ, 467, 38
- [20] de Lapparent, V., Galaz, G., Bardelli, S., Arnouts, S., 2003, A&A accepted, astro-ph/0301339
- [21] Le Fevre, O., et al., 1999, ASP, Vol. 176, 250
- [22] Lilly, S., Tresse, L., Hammer, F., Crampton, D., Le Fevre, O., 1995, ApJ, 455, 108
- [23] Madgwick, D. S., et al. (*the 2dFGRS Team*) 2002, MNRAS, 333, 133
- [24] Madgwick, D. S., Somerville, R., Lahav, O., Ellis, R. S., 2003, MNRAS, submitted
- [25] Roweis, S., 1997, Neural Info. Proc. Sys. 10, 626
- [26] Scalo, J. M., 1986, Fund. Cos. Phys., 11, 1
- [27] Slonim, N., Somerville, R., Tishby, N., Lahav, O., 2001, MNRAS, 323, 270
- [28] Somerville, R. S., Primack, J. R., 1999, MNRAS, 310, 1087
- [29] Strateva, I., et al. (*the SDSS Collaboration*) 2001, AJ, 122, 1862
- [30] Strauss, M. A., et al. (*the SDSS Collaboration*), 2002, AJ, 124, 1810
- [31] Tipping, M. E., Bishop, C. M., 1999, J. Royal Statistical Soc., Series B, 61, 611
- [32] Weiner, B., et al., (*the DEEP2 Team*) 2003, in preparation
- [33] Willmer, C. N. A., et al., (*the DEEP2 Team*) 2003, in preparation

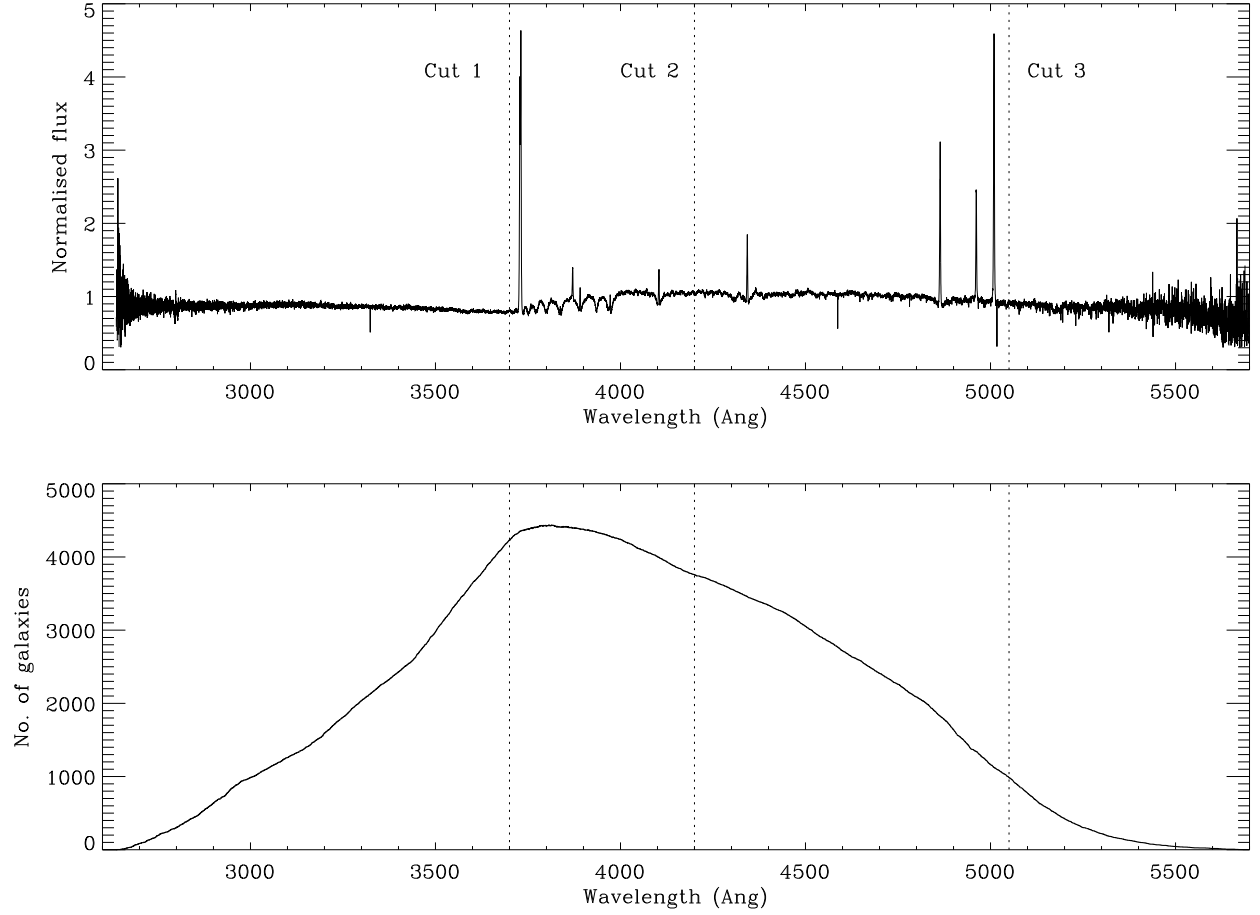


FIG. 1.— The mean rest-frame spectrum for all galaxies ($z > 0.6$) observed to date in the DEEP2 Redshift Survey. The top panel shows the mean spectrum in units of normalized flux, while the bottom panel shows how many galaxies have contributed to each wavelength channel (which is determined by the redshift and wavelength coverage of each galaxy). Also shown (dotted lines) are the wavelength ranges considered in our PCA analyses, one spans Cut1 to Cut 2 (3700 – 4200Å), the second Cut 1 to Cut 3 (3700 – 5050Å).

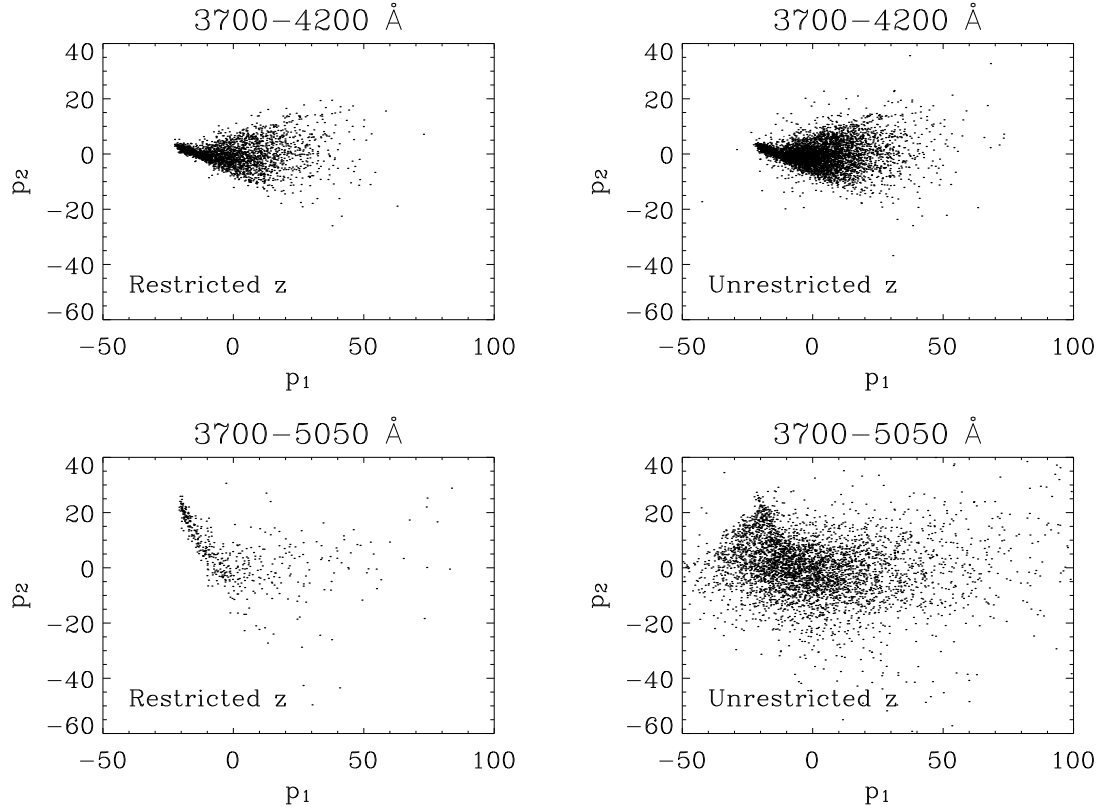


FIG. 2.— The first two projections (p_1 and p_2) are shown for both the PCA analyses. The top two panels show the projections for the PCA defined using only the 3700–4200 Å wavelength range, while the bottom cover 3700–5050 Å. In each case the left panel shows the projections for only those galaxies which span the full rest-frame wavelength range used, whereas the right panel shows the projections for all DEEP2 galaxies, regardless of their restframe wavelength coverage. It can be seen that the PCA is consistent in both samples for the shorter wavelength range adopted, but not for the larger range. This is also found to be true of higher principal components p_3 , p_4 etc.

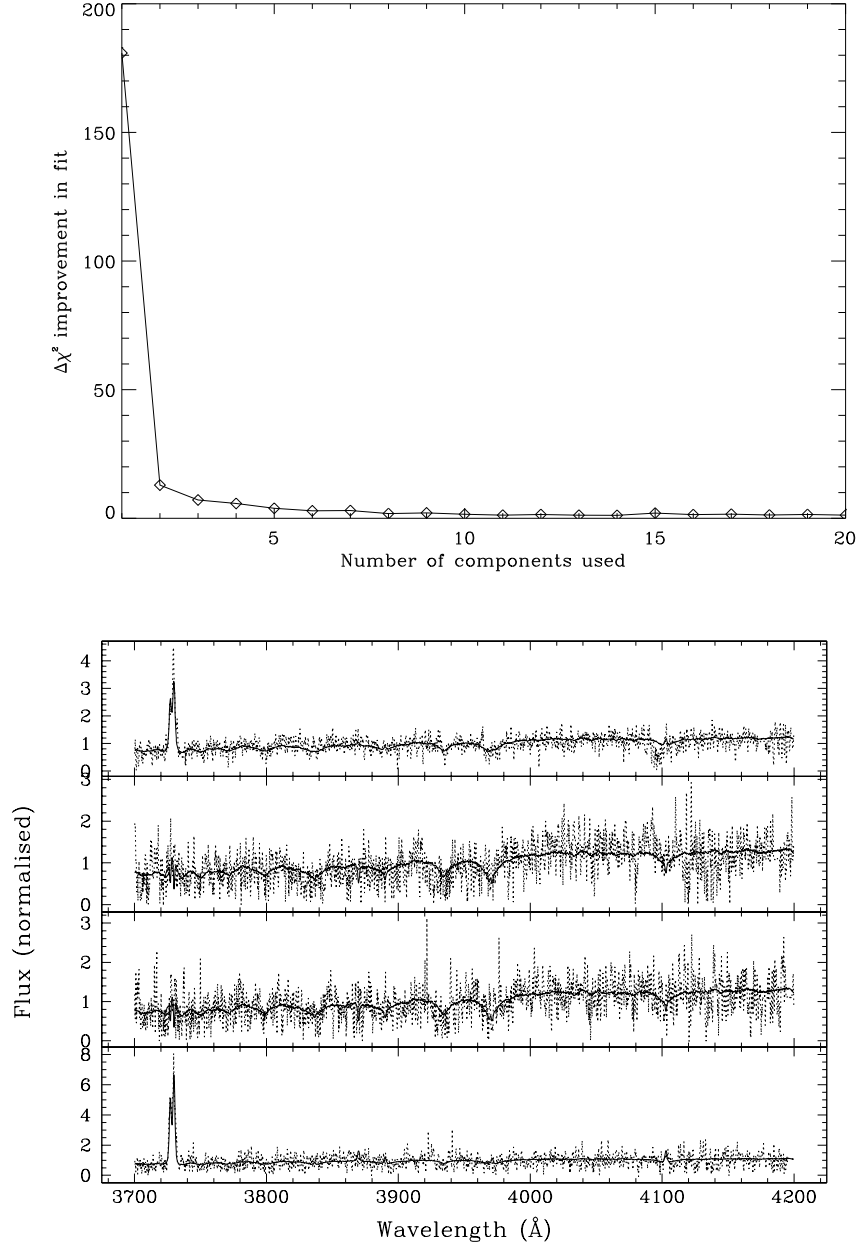


FIG. 3.— The significance of each principal component is shown in the top panel, where the improvement in the χ^2 difference between the galaxy spectrum, $f'(\lambda)$, and its reconstruction from the first i components, $\sum_i p_i \mathbf{P}_i$ has been plotted for increasing i . The lower panel shows how well a set of randomly chosen galaxy spectra (dotted lines) can be reconstructed using only the mean DEEP2 spectrum and the first principal component, p_1 (solid lines). This highlights the fact that although \mathbf{P}_1 appears to only encapsulate information about the nebular emission features (Fig. 4), it does in fact also contain enough information to reconstruct galaxy spectra without these features.

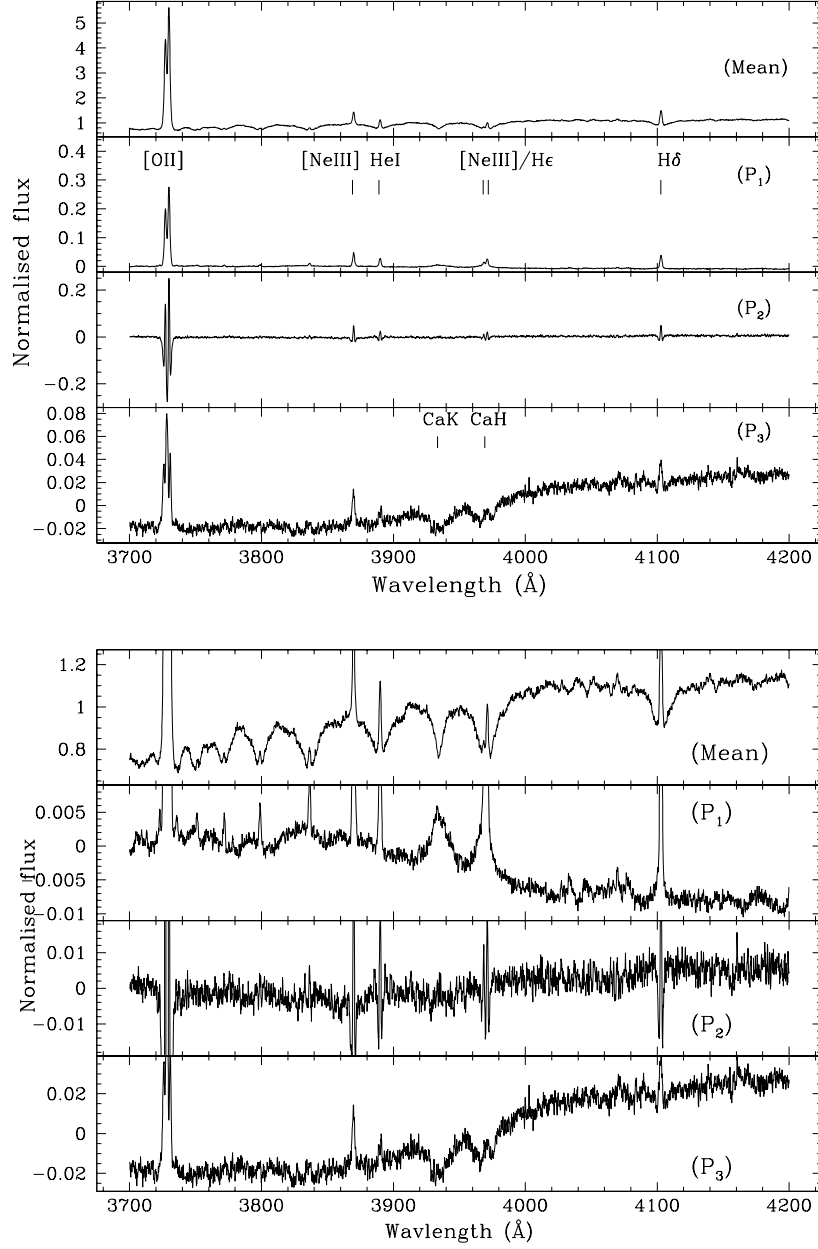


FIG. 4.— The first three eigenvectors (eigenspectra) derived from the 3700-4200Å PCA are shown (top plot), together with the mean of the DEEP2 spectra. The first, P_1 , appears to be dominated by the strength of any emission lines present. The second displays artifacts from the varying width of these emission features, while the third appears to measure the amplitude of the 4000Å break. Note that these eigenspectra have been derived from the mean subtracted galaxy spectra, and hence represent the difference between each galaxy spectrum and the mean spectrum (top panel). The lower plot shows a close-up view of the continuum of the mean spectrum and that of the first 3 eigenspectra, in which it can be seen that P_1 also contains an anti-correlation with the absorption features in each spectrum. It can also be seen how each component adds successively less information about the features present in each spectrum.

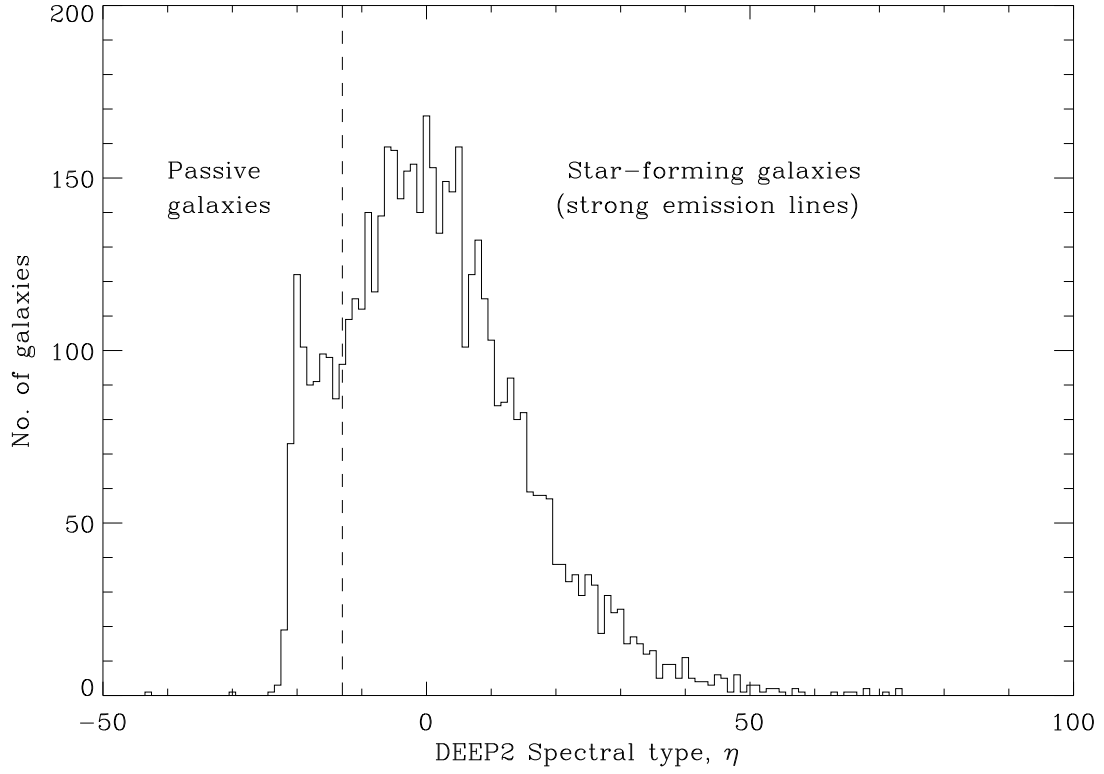


FIG. 5.— The distribution of spectral types, $\eta \equiv p_1$, is shown for all the galaxies observed to date in the DEEP2 Redshift Survey. It can be seen that there is a slight bimodality about $\eta = -13$ and for this reason we adopt a division of our galaxies at this point.

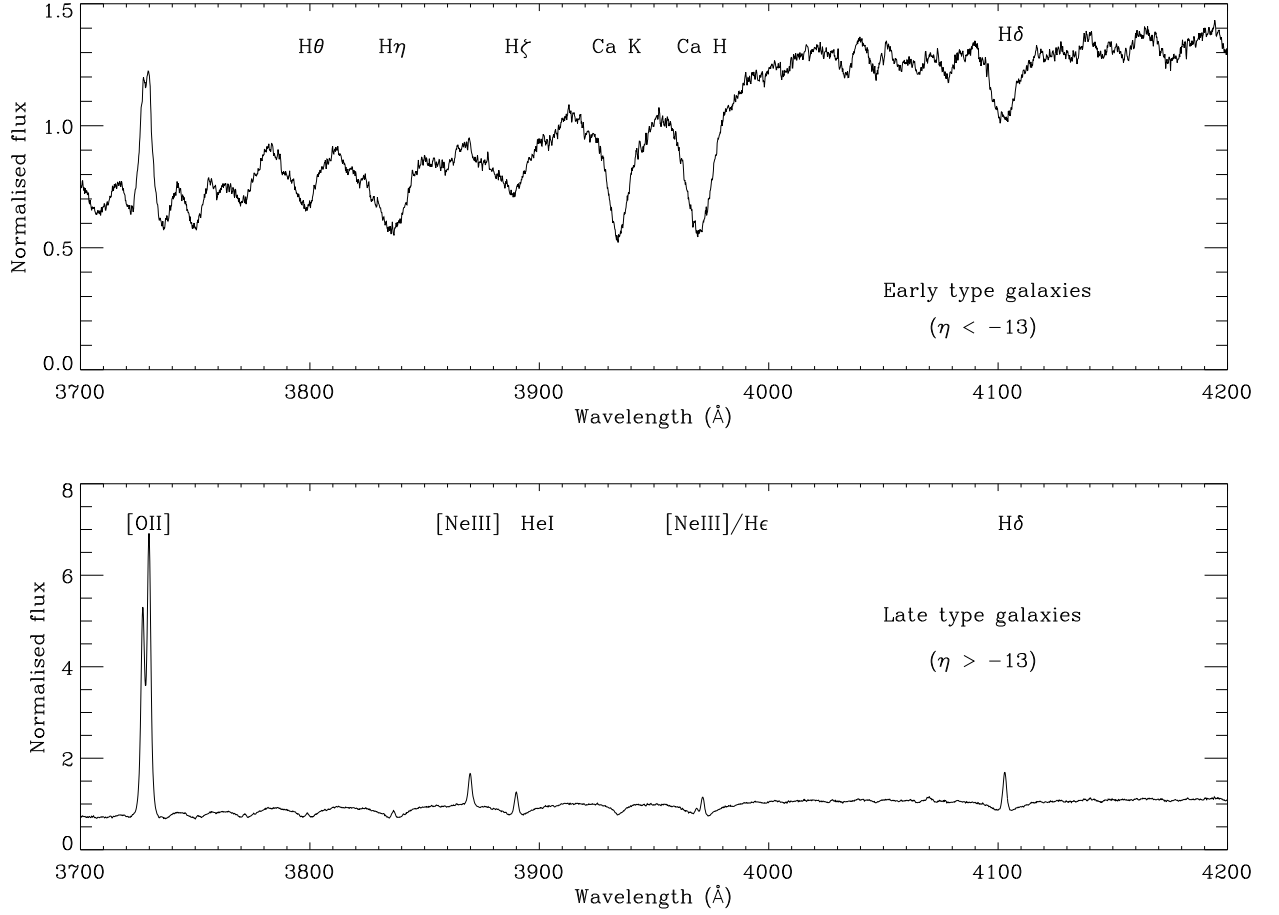


FIG. 6.— The average spectrum of the two different ‘types’ of galaxies are shown, again in terms of normalized flux. It can be seen that the PCA has been very successful at separating different types of galaxy spectra.

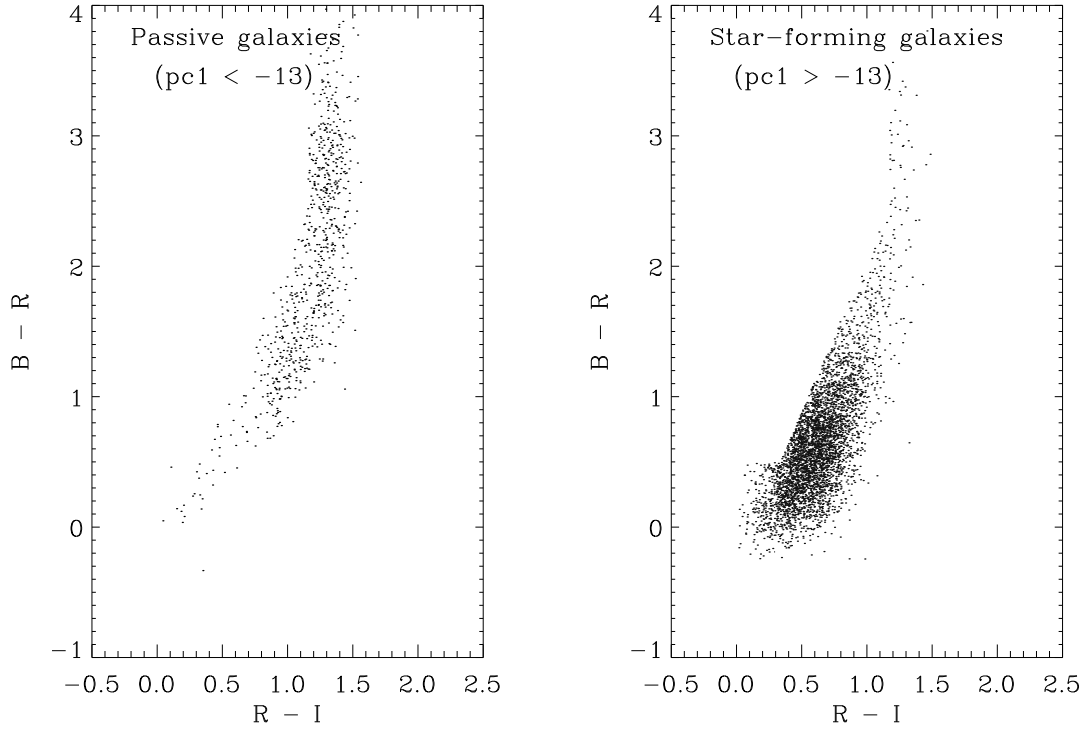


FIG. 7.— The distribution of observed $(R - I)$ and $(B - R)$ colors are shown for both types of galaxy. It can be seen that there is a very good separation between the different galaxy types in the observed color distribution.

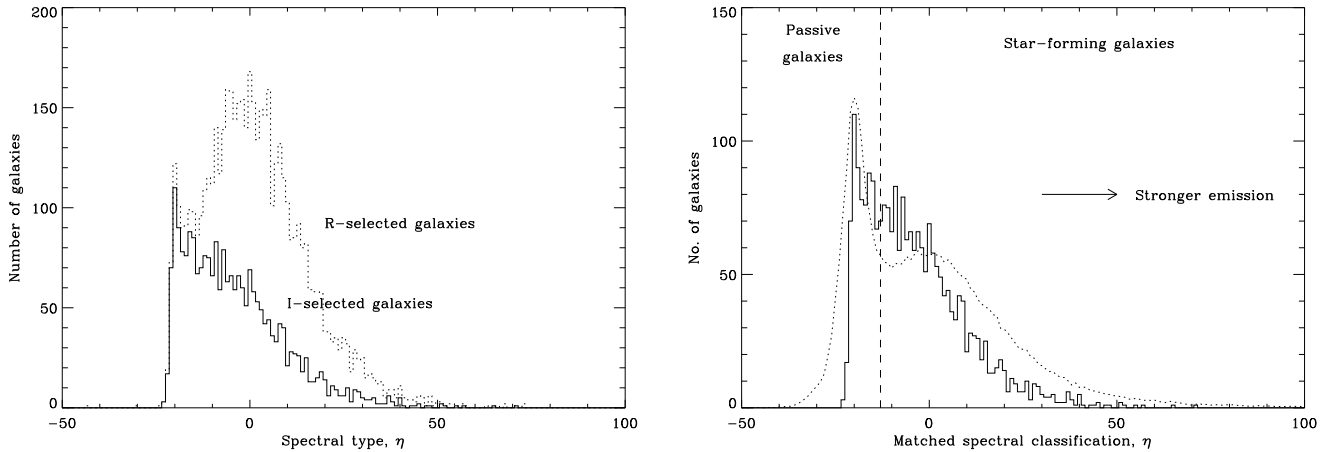


FIG. 8.— Comparison between classifications in the DEEP2 Survey and the 2dFGRS. The left panel compares the distribution of spectral types in the DEEP2 Survey using either an R or I -limited sample. Over the redshift interval under consideration ($0.7 < z < 1.0$) these two samples correspond to restframe U or B selection respectively. The right panel compares the distribution of spectral types in the 2dFGRS with the I -selected subsample of DEEP2, both of which should correspond to a restframe B selection of galaxies. It has been shown previously that the spectral type, η , is closely correlated with star-formation activity in each galaxy, from which we can conclude that restframe U selection greatly increases the relative fraction of star-forming galaxies in the DEEP2 sample.

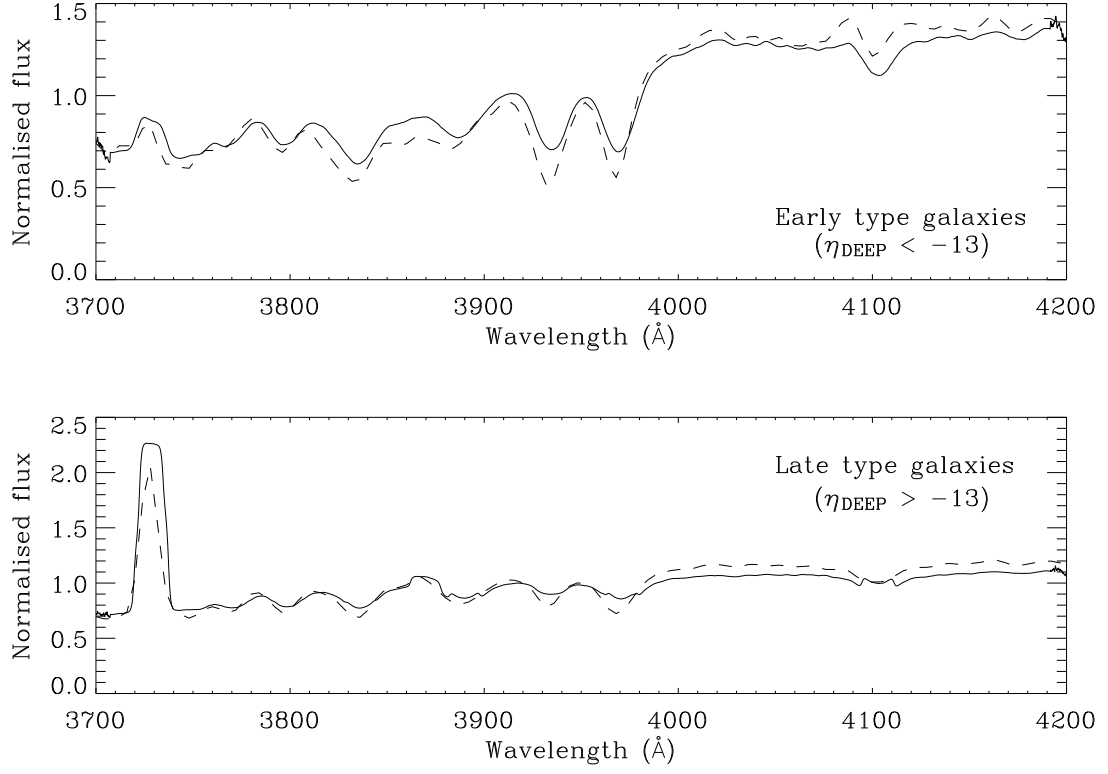


FIG. 9.— The average spectrum of the early and late type galaxies from the 2dFGRS and DEEP2 surveys are compared. The DEEP2 galaxy spectra (solid line) have been smoothed using an 8 Å filter in order to match the resolution of the 2dFGRS spectra.